Desalination and Water Treatment
www.deswater.com

doi:10.5004/dwt.2017.0216

72 (2017) 190–196
April

Sol-gel synthesis of χTiO_2/HZSM-5 and photocatalytic degradation of phenol

Wenjie Zhang[a,*], Zheng Ma[a], Xijuan Chen[a,b], Hongbo He[b]

[a]*School of Environmental and Chemical Engineering, Shenyang Ligong University, Shenyang 110159, China, Tel. +86 24 24680345, email: wjzhang@aliyun.com (W. Zhang), believezhuan@163.com (C. Li); chenxj@iae.ac.cn (X. Chen),*
[b]*State Key Laboratory of Forest and Soil Ecology, Institute of Applied Ecology, Chinese Academy of Sciences, Shenyang 110164, China, email: hehongbo@iae.ac.cn (Hongbo He)*

Received 21 February 2016; Accepted 23 June 2016

ABSTRACT

Composite χTiO_2/HZSM-5 photocatalysts were prepared by a sol-gel method and were used for photocatalytic degradation of phenol in aqueous solution. The external surface of HZSM-5 is coated with a layer of TiO_2 with different thickness, according to TiO_2 loading content. Anatase TiO_2 is found in both pure TiO_2 and the supported χTiO_2/HZSM-5, while crystallite size of TiO_2 becomes smaller after loading. The supported χTiO_2/HZSM-5 has enlarged surface area that is in accordance to the content of HZSM-5. The 50% TiO_2/HZSM-5 sample has the maximum photocatalytic activity, on which total degradation of phenol molecules in the solution is achieved after 120 min of irradiation. At the same time, organic groups in phenol molecules are thoroughly degraded into inorganic substances, which are proved by UV-Vis absorption spectra, FT-IR spectra and TOC analyses.

Keywords: Sol-gel; TiO_2; HZSM-5; Photocatalytic

1. Introduction

TiO_2 based materials are widely studied in the environmental cleaning process using photocatalytic oxidation technique [1–3]. After decades of investigation in this promising area, the materials have gradually been applied to deal with various environmental problems such as wastewater treatment [4]. However, large scale industrial plant has to solve the problem of separating photocatalyst from the treated wastewater. Since filtration of very fine powders from water is not easy, the supported forms are studied for the potential industrial application.

Some kinds of materials such as graphite [5], SiO_2 [6] and glass [7] are used to support TiO_2. Adsorption of pollutants on the supported form is beneficial to concentrate pollutants on photocatalyst's surface [8,9]. Literatures also reported the positive effects of interactions between TiO_2 and the supports on photocatalytic activity of TiO_2 [10–12]. Synthesized zeolite is used as industrial adsorbent and catalyst, owing to the porous structure and large surface area of this kind of material. The unique Si-Al skeleton in zeolite is involved in electron transfer process that makes it possible to support TiO_2-based photocatalyst [13–15].

Although some kinds of zeolites such as MCM-41 [16], HY [17], ZSM-5 [18,19] and clinoptilolite [20] were reported as supports for TiO_2, it is worthy of studying the application of such composite materials on decomposing environmentally concerned pollutants. In this work, composite χTiO_2/HZSM-5 photocatalysts were prepared by a sol-gel method for the purpose of photocatalytic degradation of phenol. Attention was paid to the photocatalytic degradation of phenol on χTiO_2/HZSM-5 with respect to TiO_2 weight percentage and irradiation time. Intermediates and residues in the phenol solution during degradation were determined using FT-IR, UV-Vis spectrum and TOC analyses.

2. Experimental

2.1. Synthesis of χTiO_2/HZSM-5

Zeolite NaZSM-5 in the n(Si)/n(Al) ratio of 100 was provided by Nankai Catalyst Corporation in China. The raw NaZSM-5 powders were treated in 0.5 mol/L phos-

*Corresponding author.

phoric acid solution to prepare HZSM-5 through Na^+–H^+ exchanging.

HZSM-5 supported TiO_2 photocatalysts were prepared by a sol-gel method. 2 mL tetrabutyl titanate, 0.04 mL acetylacetone, 0.1 mL hydrochloric acid, 6 mL anhydrous ethanol and HZSM-5 were mixed together. Another mixture containing 0.6 mL deionized water and 3 mL anhydrous ethanol was slowly added to the former slurry. Tetrabutyl titanate was hydrolyzed on the surface of HZSM-5 to form a gel. The gel was dried at 80°C for 7 h, and then calcinated at 400°C for 2 h. The produced materials were ground into fine powder and named as χTiO_2/HZSM-5, where χ means the weight percentage of TiO_2 in the composite photocatalyst. A serious of samples was synthesized in different weight percentage of TiO_2 and the representative samples were discussed later.

2.2. Characterization of the materials

X-ray diffraction patterns of the materials were measured using D/max-rB with a Cu Kα source. Lattice parameters were calculated from XRD data using the analytical software Jade 5.0. The surface morphology was observed by QUANTA 250 scanning electron microscope at an accelerating voltage of 30 kV. The working distance was 7.2 mm. A thin layer of gold was coated on the samples to avoid charging. An F-Sorb 3400 instrument was used to measure specific surface area and porosity of the materials at –196°C. The specific surface area was determined by the multipoint BET method using the adsorption data in the relative pressure (P/P_o) range of 0.05–0.25. The desorption isotherm was used to determine pore size distribution using the Barrett, Joyner, and Halenda (BJH) method.

2.3. Degradation of phenol

Photocatalytic degradation of phenol was conducted in a lab-made quartz reactor. A 20 W UV lamp was located over a 100 mL column-sized quartz reactor in the distance of 15 cm. The lamp can irradiate UV light at wavelength of 253.7 nm with the intensity of 1200 μW/cm^2. The initial phenol concentration was 20 mg/L. 50 mL phenol solution and 10 mg TiO_2 were mixed in the reactor. In prior to turn on the lamp, the solution was magnetically stirred for 25 min to ensure adsorption-desorption equilibrium in the dark. The suspensions were filtrated through a Millipore filter (pore size 0.45 μm) to remove the photocatalyst before measuring.

Phenol concentration was measured at the wavelength of 270 nm using an Agilent 1260 HPLC with a C_{18} column at 30°C. The mobile phase was composed of 60% ethane and 40% ultrapure water at a flow rate of 1 mL/min. Intermediates and residues in the phenol solution during degradation were determined using FT-IR and UV-Vis spectrophotometers. Total organic carbon in the solution was measured using a multi N/C 3100 TOC analyzer.

3. Results and discussion

3.1. Characterization of the materials

Fig. 1 shows surface morphologies of HZSM-5, TiO_2 and χTiO_2/HZSM-5. HZSM-5 is normally composed of regular shaped particles with comparatively smooth surface. A typical HZSM-5 particle is usually as large as 5 μm. Pure TiO_2 is composed of rough and small particles in the size below 2 μm. As can be seen in Fig. 1b–e, TiO_2 is coated on the surface of HZSM-5 so that the shape of HZSM-5 cannot be distinguished in the composite χTiO_2/HZSM-5. The external surface of HZSM-5 is coated with a layer of TiO_2 in different thickness, depending on loading content of TiO_2. The dispersion of TiO_2 on the surface of HZSM-5 inhibits particles growing and aggregation as in the case of pure TiO_2. The surfaces of the supported χTiO_2/HZSM-5 are fairly rough as the result of scattering of TiO_2 small particles.

XRD patterns of HZSM-5, TiO_2 and χTiO_2/HZSM-5 are shown in Fig. 2. The major diffraction peaks of HZSM-5 zeolite can be distinguished in the patterns of the supported χTiO_2/HZSM-5, although peak intensities of HZSM-5 drop off with rising TiO_2 loading content. The typical diffraction peaks of anatase TiO_2 can be found in the patterns of both pure TiO_2 and the supported χTiO_2/HZSM-5. The most preferred orientation of anatase TiO_2 appears at $2\theta = 25.1°$, which is related to [101] plane of anatase crystallite TiO_2 in JCPDS 211272 card. There are no signals of other TiO_2 phase in the diffraction patterns due to the low calcination temperature in preparation of the materials.

The [101] plane of anatase TiO_2 is used to calculate crystallite size of TiO_2, according to Scherrer formula, $L = K\lambda/(\beta \cdot \cos\theta)$. The pure TiO_2 is composed of crystals in the average size of 15.4 nm. The crystallite sizes of TiO_2 in 30%TiO_2/0.5HZSM-5, 50%TiO_2/0.5HZSM-5, 70%TiO_2/0.5HZSM-5 and 90%TiO_2/0.5HZSM-5 are 12.1, 12.3, 12.9 and 14 nm, respectively. The distribution of TiO_2 on the surface of HZSM-5 particles is beneficial to the shrinking crystallite size, probably due to restricted aggregation of TiO_2 crystals after loading.

Table 1 gives specific surface area and porous parameters of HZSM-5, χTiO_2/HZSM-5 and TiO_2. The BET surface area of HZSM-5 is as high as 273.6 m^2/g, due to its three dimensional cave structure. The supported χTiO_2/HZSM-5 has enlarged surface area as compared to pure TiO_2 in accordance to the increasing content of HZSM-5. Obviously, TiO_2 is loaded on the external surface of HZSM-5 without blocking the micropores inside the zeolite, since the internal micropores in HZSM-5 contributes the majority of surface area in the supported χTiO_2/HZSM-5.

Both of pure and the supported TiO_2 samples contain a large amount of mesopores as the result of crystals aggregation during synthesizing process. The average pore size in pure TiO_2 is 16.9 nm and the total pore volume is 0.1450 cm^3/g. Since cave diameter in HZSM-5 is usually below 1 nm, the average pore size of HZSM-5 particles is only 3.3 nm although there are still many larger interparticle pores in the HZSM-5 powder. However, 10%TiO_2/HZSM-5 has an average pore size of 12.3 nm despite 90% of HZSM-5 in the composite material. TiO_2 particles disperse on the external surface of HZSM-5 particles after loading, and may also aggregate to form a large amount of mesopores and interparticle macropores.

3.2. Photocatalytic degradation of phenol solution

Fig. 3 shows photocatalytic degradation of phenol solution with the variation of TiO_2 loading content in χTiO_2/

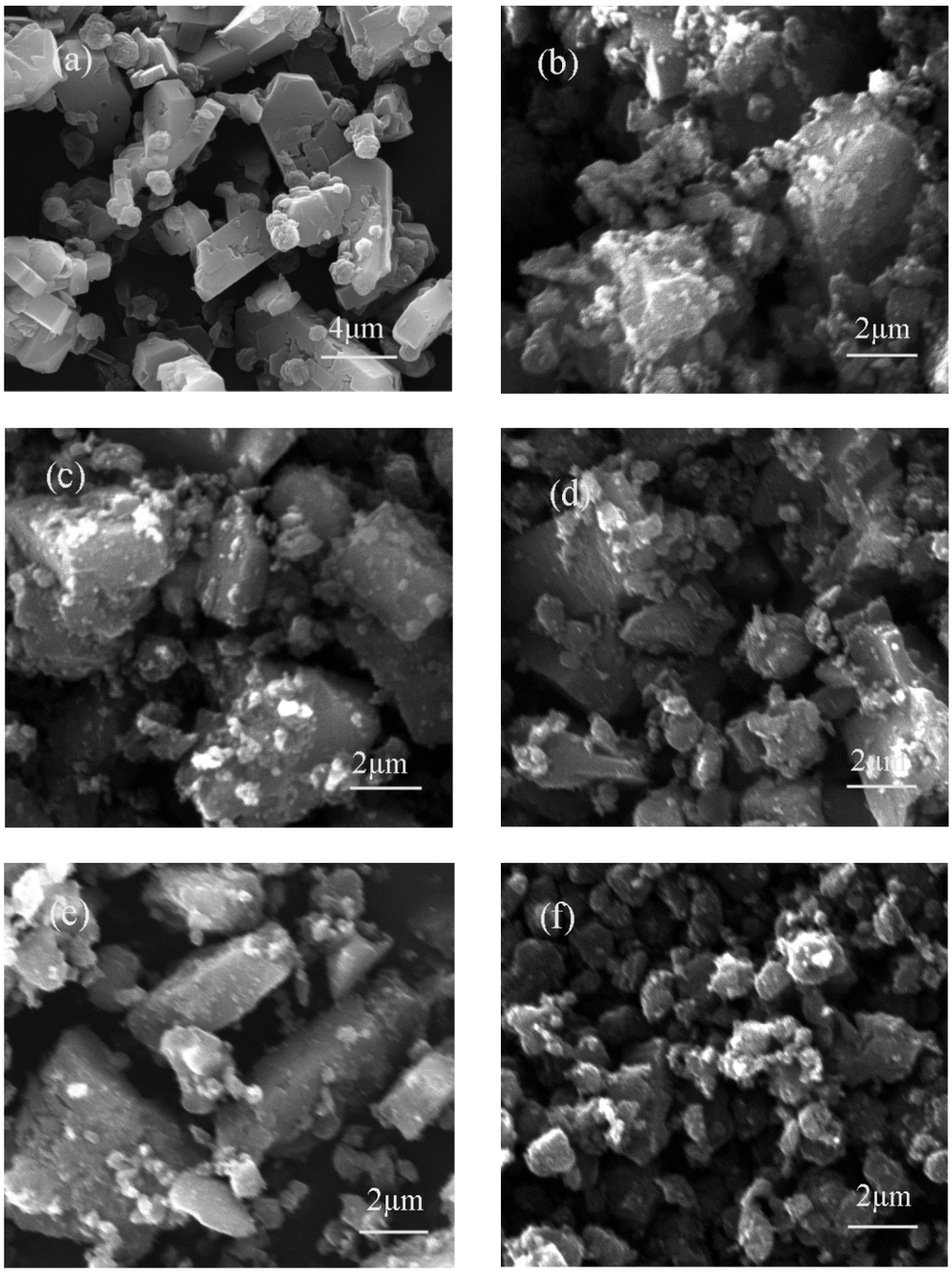

Fig. 1. SEM images of HZSM-5, χTiO_2/HZSM-5 and TiO_2. (a) HZSM-5, (b) 10% TiO_2/HZSM-5, (c) 30% TiO_2/HZSM-5, (d) 50% TiO_2/HZSM-5, (e) 70% TiO_2/HZSM-5, (f) TiO_2.

HZSM-5. Adsorption-desorption equilibrium was reached in prior to turn on the light. Both the HZSM-5 and TiO_2 can hardly adsorb phenol molecules. HZSM-5 has no photocatalytic activity on phenol degradation under UV irradiation. Phenol can be slowly photolyzed under the irradiation of UV light, while the photodissociation efficiency is only 5% after 90 min. Photocatalytic oxidation can lead to faster decomposition of phenol, depending on the type of photocatalyst in the solution. TiO_2 exhibits enhanced photocatalytic activity after loading on HZSM-5. The dispersion of TiO_2 on the external surface of HZSM-5 is the key factor in phenol degradation. Although the same amount of TiO_2 is used in the solution, specific surface area of TiO_2 is enlarged after supporting. Both the absorption of impinging photons and the adsorption of phenol molecules are enhanced consequently. As stated before, the distribution of TiO_2 on the surface of

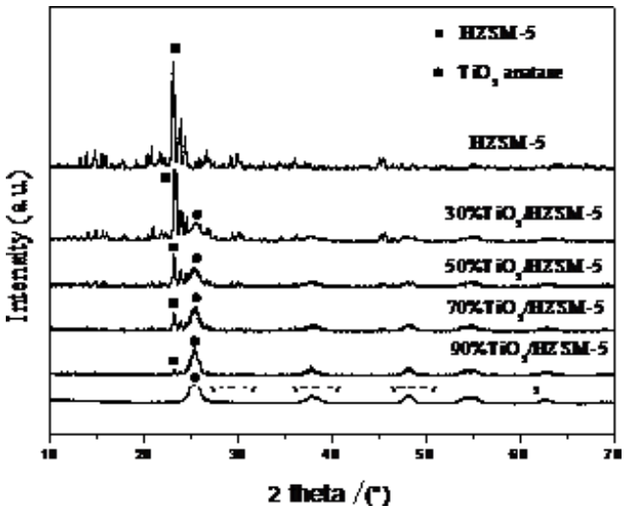

Fig. 2. XRD patterns of HZSM-5, TiO2 and χTiO_2/HZSM-5.

Table 1
Specific surface area, average pore size and total pore volume of HZSM-5, χTiO_2/HZSM-5 and TiO_2

Samples	BET surface area (m^2/g)	Average pore size (nm)	Total pore volume (cm^3/g)
HZSM-5	273.6	3.3	0.1702
10%TiO_2/HZSM-5	243.9	12.3	0.1938
30%TiO_2/HZSM-5	199.6	12.5	0.1961
50%TiO_2/HZSM-5	168.3	14.8	0.1998
70%TiO_2/HZSM-5	98.1	16.2	0.1902
TiO_2	87.9	16.9	0.1450

HZSM-5 particles leads to shrinking crystallite size, which is usually beneficial to photocatalytic degradation efficiency.

The 50%TiO_2/HZSM-5 sample has the maximum activity. Total photocatalytic degradation of phenol molecules in the solution happens on 50%TiO_2/HZSM-5 after 120 min of irradiation. Photocatalytic activity of χTiO_2/HZSM-5 is continuously enhanced when TiO_2 loading content rises up to 50%. Subsequently, an obvious decline of activity can be found for 70%TiO_2/HZSM-5 that contains 70% TiO_2. The excessive HZSM-5 particles in the samples with low TiO_2 content might inhibit absorption of UV irradiation by the supported TiO_2. On the other hand, a necessary amount of HZSM-5 particles is needed for thorough dispersion of TiO_2 on the surface of HZSM-5, so that photocatalytic activity drops off when TiO_2 content exceeds the optimal value. *E*g value of the unsupported TiO_2 is around 3.18 eV, while the χTiO_2/HZSM-5 samples have slightly smaller *E*g values. Since the major irradiating wavelength is 253.7 nm in this work, the minor variation in *E*g value will not have noticeable effect on degradation efficiency.

The reusability of 50%TiO_2/HZSM-5 in phenol degradation was also studied. Degradation efficiency decreases gradually after recycles. The suspensions were filtrated through the Millipore filter (pore size 0.45 μm) to remove the photocatalyst after each photocatalytic reaction cycle. Fine photocatalyst particles are lost during washing, filtrating and drying in each cycle, leading to continuing dropping of photocatalytic activity. Total phenol degradation efficiency decreases from 100% to 93.5% on 50%TiO_2/HZSM-5 after 5 reaction cycles.

The removal of total organic carbon (TOC) in phenol solution during irradiation is shown in Fig. 4. The TOC removal efficiency is in accordance to photocatalytic activity of χTiO_2/HZSM-5 with the variation of TiO_2 content. All the supported χTiO_2/HZSM-5 samples can remove the organic carbons in the solution much faster than pure TiO_2. The maximum TOC removal efficiency occurs in the solution using 50%TiO_2/HZSM-5, on which all the organic

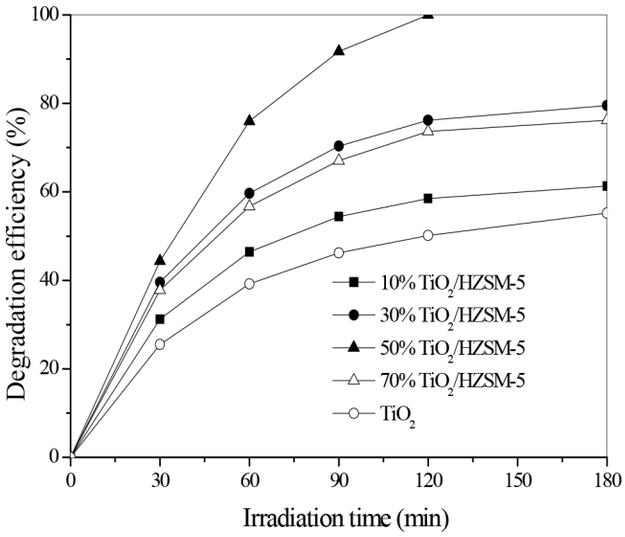

Fig.3 Degradation of phenol solution on TiO_2 and χTiO_2/HZSM-5 under UV light irradiation.

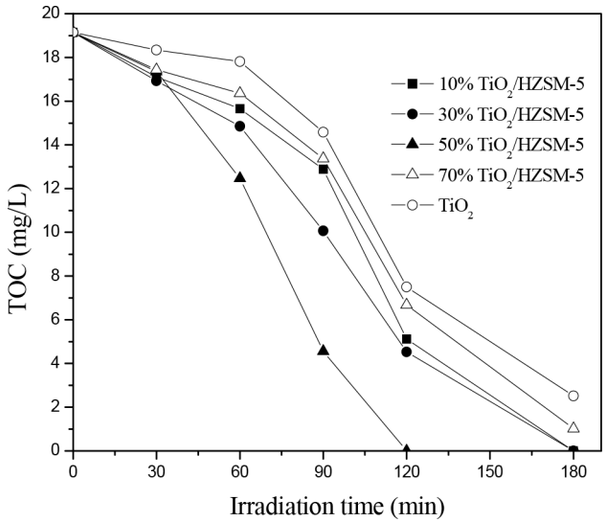

Fig. 4 TOC removal in phenol solution containing TiO_2 and χTiO_2/HZSM-5 photocatalysts during irradiation.

carbon is degraded after 120 min of irradiation. Phenol can be totally converted into inorganic products without leaving any organic residues in the solution. Organic substances under the attack of photogenerated oxidative species will firstly be broken up to form smaller intermediates whose organic carbons can still be measured. The organic substances coming from decomposition of phenol molecules can in turn be converted into inorganic products.

3.3. UV-Vis and FT-IR spectra of phenol solution during degradation

Fig. 5 shows UV-Vis absorption spectra of phenol solution during degradation on TiO_2 and χTiO_2/HZSM-5. The spectrum of phenol has three major absorption peaks situating at 196 nm, 213 nm and 268 nm in the ultraviolet region. The first two peaks are attributed to the characteristic absorption of benzene ring in phenol molecule. The

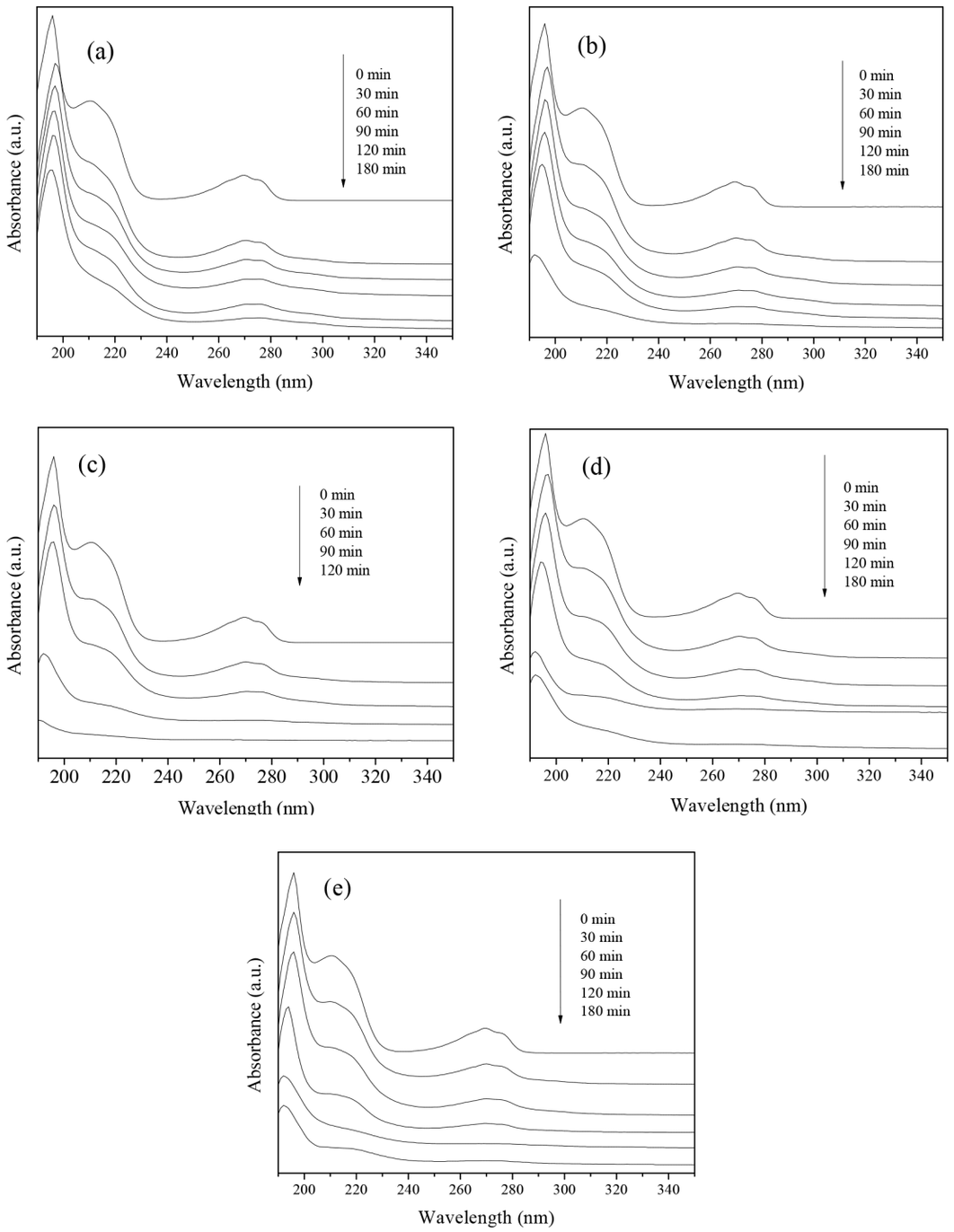

Fig. 5. UV-Vis absorption spectra of phenol solution during degradation on TiO_2 and χTiO_2/HZSM-5. (a) 10% TiO_2/HZSM-5, (b) 30% TiO_2/HZSM-5, (c) 50% TiO_2/HZSM-5, (d) 70% TiO_2/HZSM-5, (e) TiO_2.

absorption intensities of these two peaks decrease continuously with extending irradiating time, showing the breaking up of benzene ring during photocatalytic oxidation process. The peak at 210 nm moves to about 220 nm with extending irradiation time, indicating the formation of an intermediate substance, dihydroxybenzene. However, the absorption of dihydroxybenzene also disappears afterwards. The peak at 268 nm is the characteristic absorption of hydroxyl group in phenol molecule, which gradually shrinks during degradation and disappears after a certain time. As can be seen in Fig. 4c, nearly no absorption of the solution can be found in the UV region after 120 min of irradiation, while there are still apparent absorptions in the other spectra. Obviously, the benzene ring in phenol molecules can be degraded much faster when 50%TiO_2/HZSM-5 is applied as the photocatalyst.

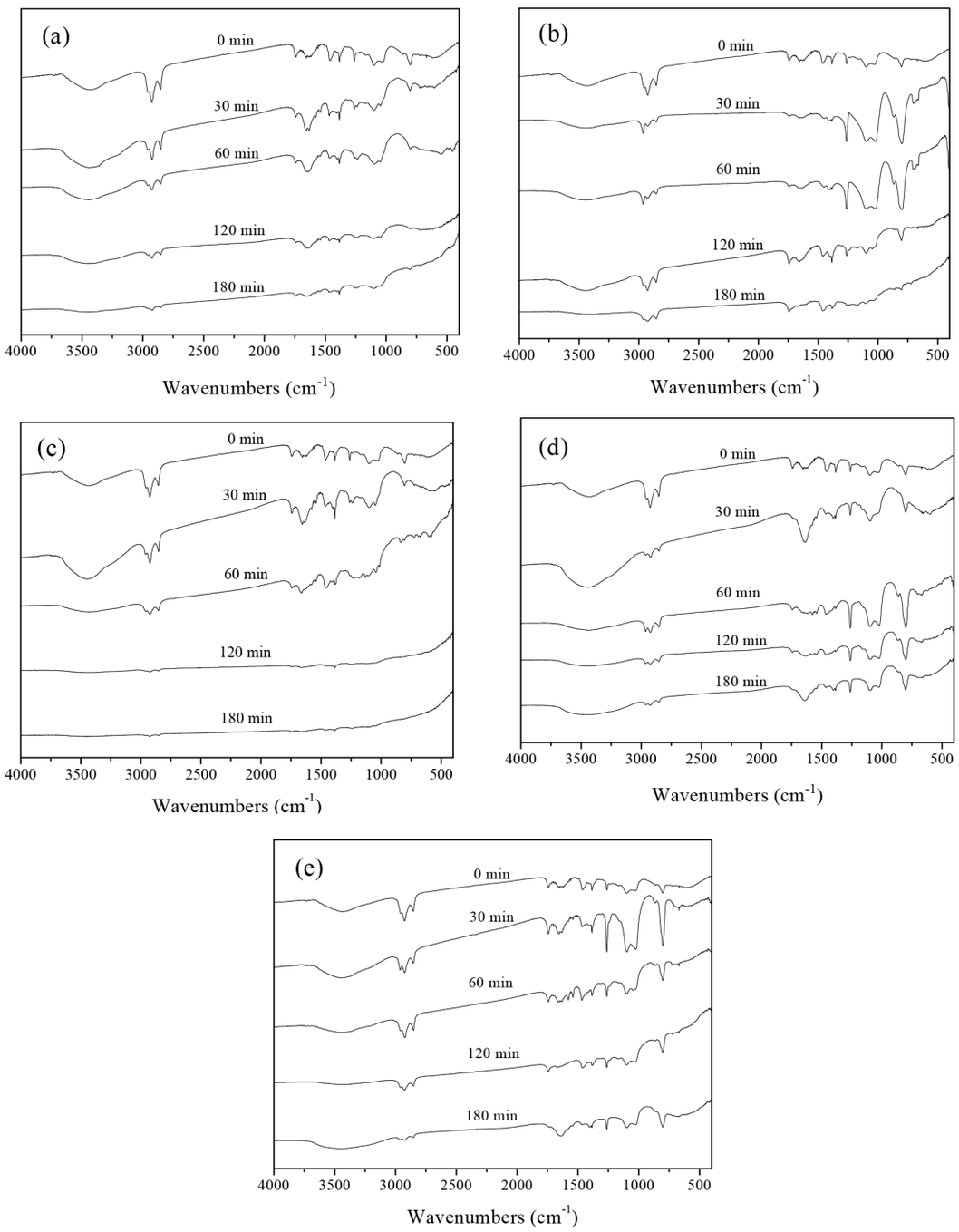

Fig. 6. FT-IR spectra of phenol solution during degradation on TiO_2 and χTiO_2/HZSM-5. (a) 10% TiO_2/HZSM-5, (b) 30% TiO_2/HZSM-5, (c) 50% TiO_2/HZSM-5, (d) 70% TiO_2/HZSM-5, (e) TiO_2.

Fig. 6 shows FT-IR spectra of phenol solution during degradation with the existence of TiO_2 and χTiO_2/HZSM-5. In the FT-IR spectra of the initial phenol solution, the absorption peaks at 3400 cm^{-1} and 1250 cm^{-1} are the stretching and bending vibrations of O–H in phenol molecule. The C-C stretching vibrations are in the region between 1400 cm^{-1} and 1650 cm^{-1}, among which the absorptions at 1625 cm^{-1}, 1548 cm^{-1}, 1493 cm^{-1}, 1458 cm^{-1} and 1418 cm^{-1} are attributed to benzene ring.

The above mentioned organic groups in phenol can be degraded under photocatalytic oxidation. Photo-generated electrons and holes can lead to the formation of hydroxyl radicals and other oxidative species, which will lead to the breakup of benzene rings. As stated before, TiO_2 loading content in the composite χTiO_2/HZSM-5 is a key factor influencing photocatalytic degradation efficiency. As can be seen from the figure, the absorption intensities of all the peaks in Fig. 6c decrease much faster than those in the other figures, demonstrating the optimal photocatalytic activity of 50%TiO_2/HZSM-5. Nearly no absorption intensity can be measured in the solution after 120 min of irradiation when 50%TiO_2/HZSM-5 is used. That means the organic groups in phenol molecules are thoroughly degraded into inorganic substances, which is also proved by TOC analyses.

The degradation mechanism of phenol can be concluded as a conjecture. Phenol molecule is attacked by hydroxyl radical in the initial step to form an intermediate, dihydroxybenzene. Dihydroxybenzene can be oxidized to form benzoquinone. Subsequently, the breaking up of benzene ring and oxidation of hydroxyl group leads to degradation of the intermediates into smaller molecules such as aldehyde and carboxylic acid. The organic substances can be mineralized into carbon dioxide and water at the end.

4. Conclusions

Anatase TiO_2 was supported on HZSM-5 by a sol-gel method to evaluate the effects of TiO_2 loading content on photocatalytic degradation of phenol. TiO_2 is loaded on the external surface of HZSM-5 without blocking the micropores inside the zeolite, so that the specific surface area of the supported χTiO_2/HZSM-5 is much larger than pure TiO_2. Photocatalytic activity of χTiO_2/HZSM-5 is continuously enhanced when TiO_2 loading content rises up to 50%. The results of UV-Vis absorption spectra, FT-IR spectra and TOC analyses demonstrate the thorough decomposing of phenol molecules and total removal of organic substances in the solution using 50%TiO_2/HZSM-5 as the photocatalyst.

Acknowledgments

This work was supported by the Natural Science Foundation of Liaoning Province (No. 2015020186), the National Natural Science Foundation of China (No. 41271251), and the open research fund of Key Laboratory of Wastewater Treatment Technology of Liaoning Province, Shenyang Ligong University (No. 4771004kfs38).

References

[1] D. Chatterjee, S. Dasgupta, Visible light induced photocatalytic degradation of organic pollutants, J. Photochem. Photobiol., C 6 (2005) 186–205.
[2] M.R. Hoffmann, S.T. Martin, W. Choi, W. Bahnemann, Environmental applications of semiconductor photocatalysis, Chem. Rev., 95 (1995) 69–96.
[3] A. Fujishima, T.N. Rao, D.A. Tryk, Titanium dioxide photocatalysis, J. Photochem. Photobiol., C 1 (2000) 1–21.
[4] G. Plantard, T. Janin, V. Goetz, S. Brosillon, Solar photocatalysis treatment of phytosanitary refuses: Efficiency of industrial photocatalysts, Appl. Catal. B, 115–116 (2012) 38–44.
[5] Y. Wang, J. Lin, R. Zong, J. He, Y. Zhu, Enhanced photoelectric catalytic degradation of methylene blue via TiO_2 nanotube arrays hybridized with graphite-like carbon, J. Mol. Catal. A: Chem., 349 (2011) 13–19.
[6] D. Pang, L. Qiu, Y. Wang, R. Zhu, F. Ouyang, Photocatalytic decomposition of acrylonitrile with N-F codoped TiO_2/SiO_2 under simulant solar light irradiation, J. Environ. Sci., 33 (2015) 169–178.
[7] W. Zhang, J. Bai, Synthesis and photocatalytic properties of porous TiO_2 films prepared by ODA/sol-gel method, Appl. Surf. Sci., 258 (2012) 2607–2611.
[8] K. Yamaguchi, K. Inumaru, Y. Oumi, T. Sano, S. Yamanaka, Photocatalytic decomposition of 2-propanol in air by mechanical mixtures of TiO_2 crystalline particles and silicalite adsorbent: the complete conversion of organic molecules strongly adsorbed within zeolitic channels, Micropor. Mesopor. Mater., 117 (2009) 350–355.
[9] K. Tanaka, J. Fukuyoshi, H. Segawa, K. Yoshida, Improved photocatalytic activity of zeolite- and silica-incorporated TiO_2 film, J. Hazard. Mater., 137 (2006) 947–951.
[10] T.A. McMurray, P. Dunlop, J.A. Byrne, The photocatalytic degradation of atrazine on nanoparticulate TiO_2 films, J. Photochem. Photobiol., A 182 (2006) 43–51.
[11] Z.S. Guan, X.T. Zhang, Y. Ma, Y.A. Cao, J.N. Yao, Photocatalytic activity of TiO_2 prepared at low temperature by a photoassisted sol-gel method, J. Mater. Res., 16 (2001) 907–909.
[12] H. Yahiro, T. Miyamoto, N. Watanabe, H. Yamaura, Photocatalytic partial oxidation of methylstyrene over TiO_2 supported on zeolites, Catal. Today, 120 (2007) 158–162.
[13] H. Chen, A. Matsumoto, N. Nishimiya, K. Tsutsumi, Preparation and characterization of TiO_2 incorporated Y-zeolite, Colloids Surf. 157 (1999) 295–305.
[14] X. Liu, K.K Iu, J.K. Thomas, Encapsulation of TiO_2 in zeolite Y, Chem. Phys. Lett., 195 (1992) 163–168.
[15] M. Mahalakshmi, S.V. Priya, B. Arabindoo, M. Palanichamy, V. Murugesan, Photocatalytic degradation of aqueous propoxur solution using TiO_2 and H zeolite-supported TiO_2, J. Hazard. Mater., 161 (2009) 336–343.
[16] J.M. Coronado, S. Suarez, H_2S photodegradation by TiO_2/M-MCM-41 (M = Cr or Ce): Deactivation and by-product generation under UV-A and visible light, Appl. Catal. B, 84 (2008) 643–650.
[17] M.V.P Sharma, K. Lalitha, V.D Kumari, M. Subrahmanyam, Solar photocatalytic mineralization of isoproturon over TiO_2/HY composite systems, Sol. Energy Mater. Sol. Cells, 92 (2008) 332–342.
[18] R.M. Mohamed, A.A. Ismail, I. Othman, I.A. Ibrahim, Preparation of TiO_2-ZSM-5 zeolite for photodegradation of EDTA, J. Mol. Catal., A 238 (2005) 151–157.
[19] W.J. Zhang, K.L. Wang, Y. Yu, H.B. He, TiO_2/HZSM-5 nano-composite photocatalyst: HCl treatment of NaZSM-5 promotes photocatalytic degradation of methyl orange, Chem. Eng. J., 163 (2010) 62–67.
[20] M. Nikazar, K. Gholivand, K. Mahanpoor, Photocatalytic degradation of azo dye Acid Red 114 in water with TiO_2 supported on clinoptilolite as a catalyst, Desalination, 219 (2008) 293–300.